

Weighing black holes using open-loop focus corrections for LGS-AO observations of galaxy nuclei at Gemini Observatory

Richard M. McDermid^{*a}, Davor Krajnovic^b, Michele Cappellari^c, Chadwick Trujillo^a,
Julian Christou^a, Roger L. Davies^c

^aGemini Observatory, 670 N. A`ohoku Pl., Hilo, HI, USA 96720;

^bEuropean Southern Observatory, Karl-Schwarzschild-Str. 2, 85748 Garching, Germany;

^cUniversity of Oxford, Keble Road, Oxford, OX1 3RH, United Kingdom

ABSTRACT

We present observations of early-type galaxies with laser guide star adaptive optics (LGS AO) obtained at Gemini North telescope using the NIFS integral field unit (IFU). We employ an innovative technique where the focus compensation due to the changing distance to the sodium layer is made 'open loop', allowing the extended galaxy nucleus to be used only for tip-tilt correction. The purpose of these observations is to determine high spatial resolution stellar kinematics within the nuclei of these galaxies to determine the masses of the super-massive black holes. The resulting data have spatial resolution of 0.2" FWHM or better. This is sufficient to positively constrain the presence of the central black hole in even low-mass early-type galaxies, suggesting that larger samples of such objects could be observed with this technique in the future. The open-loop focus correction technique is a supported queue-observing mode at Gemini, significantly extending the sky coverage in particular for faint, extended guide sources. We also provide preliminary results from tests combining tip/tilt correction from the Gemini peripheral guider with on-axis LGS. The current test system demonstrates feasibility of this mode, providing about a factor 2-3 improvement over natural seeing. With planned upgrades to the peripheral wave-front sensor, we hope to provide close to 100% sky coverage with low Strehl corrections, or 'improved seeing', significantly increasing flux concentration for deep field and extended object studies.

Keywords: laser guide star, adaptive optics, integral field spectroscopy, black holes, stellar kinematics

1. INTRODUCTION

Super-massive black holes are suspected to reside at the heart of many, if not all, galaxies in the nearby universe¹, and are thought to be the engines that drive the powerful jets in active galactic nuclei (AGN), fueled by material accreting onto the black hole². As well as increasing the black hole's mass, this material unleashes the gravitational energy of the black hole, and is violently ejected in the form of radiation. The majority of galaxies in the nearby universe are not in such a highly active phase, making the possible presence of a super-massive black hole in these 'quiescent' galaxies much harder to determine. The large number of luminous quasars (thought to be AGN in a highly luminous phase) at higher redshifts, however, suggests that black holes are common at earlier epochs. These black holes must still exist at present times, but are presumably starved of the accreting material that fuels strong activity.

To detect these 'dormant' super-massive black holes, we must make use of the fact that their enormous gravitational pull can be felt far from the black hole itself. The so-called 'radius of influence' of a super-massive black hole is the distance from the black hole at which its gravitational influence is approximately comparable to that of its host galaxy. Inside this radius, the Keplerian potential of the black hole dominates over the galaxy, causing orbital velocities to increase sharply with decreasing distance to the black hole. Measuring the orbital velocities of stars or gas within the radius of influence can reveal the gravitational signature of the unseen super-massive black hole. More importantly, by accurately modeling these motions, it is possible to derive the most fundamental property of the black hole: its mass.

*rmcdermid@gemini.edu

2. THE ROLE OF ADAPTIVE OPTICS

To understand the orbital structure around the black hole, and hence gain an insight to the formation mechanism of the galaxy, the main issue is to spatially resolve the kinematics close to the black hole's radius of influence, which is typically only a few tenths of an arcsecond on the sky. At these scales, the Earth's atmosphere blurs the information, mixing up light from the galaxy nucleus with light from further out in the galaxy, and greatly dilutes the signature of the black hole.

Natural guide star adaptive optics (NGS-AO) on large telescopes can help overcome the limitations imposed by the Earth's atmosphere. Unfortunately, the number of nearby galaxies with appropriately bright, nearby guide stars is extremely few. 'Laser guide star' adaptive optics (LGS-AO) allows much fainter guide sources to be used, greatly increasing the fraction of the night sky available for AO-assisted observations. LGS-AO creates an artificial 'star', or reference source with which to measure the atmospheric distortion by making use of a 1km-thick layer of the Earth's atmosphere composed largely of atomic sodium, located at an altitude of around 90km – a result of meteor ablation. A powerful laser beam that has a wavelength identical to a resonant wavelength of the sodium stimulates a narrow column of gas within this sodium layer, causing it to fluoresce. As seen from the telescope, a bright star-like region of light is created high in the atmosphere, allowing the atmospheric turbulence to be measured and corrected by the AO system. A natural reference source is also needed to measure the bulk motion, or 'tip/tilt', caused by the atmosphere, as well as to monitor relative changes in focus caused by a varying sodium layer altitude. This natural source can, however, be several magnitudes fainter than is needed for correction of higher-order modes, therefore giving a much larger sky-coverage than NGS-AO.

The advent of LGS-AO opens a new era of high-spatial resolution observations from the ground. Moreover, the development of integral-field spectroscopy and infrared capabilities allow a two-dimensional region to be spectrally mapped simultaneously, whilst realizing spatial resolutions close to the theoretical limit of the telescope. This effectively gives telescopes like Gemini the spatial resolving power of the HST, whilst having an order of magnitude larger light collecting area, and a broader range of instrumental capabilities.

3. USING OPEN-LOOP FOCUS

Although LGS-AO allows fainter guide sources to be used, galaxies that may have a resolvable radius of influence tend to be nearby, and spatially extended on the sky, meaning that guide stars are either super-imposed on (and confused with) the galaxy light itself, or are positioned so far from the galaxy nucleus that the spatial resolution is degraded due to anisoplanatism (incoherence of the atmosphere between two different lines of sight or positions on the sky), rendering it ineffective.

To get around this problem, we have used a new technique at Gemini North known as the 'open-loop' focus model. Whilst the nuclei of most nearby galaxies are too faint and extended to reliably measure the telescope focus, they can still be used to determine tip/tilt. Information on the telescope focus is required to account for possible changes in the distance from the telescope to the sodium layer (at roughly 90km), which can drive the telescope out of focus for the science target (at infinity). With this technique, instead of trying to measure the focus dynamically on the galaxy nucleus, the assumed distance to the sodium layer (and therefore the telescope focus) is controlled by a so-called 'open-loop' focus model. This is a geometric model of how the distance to the sodium layer changes as the telescope tracks a target on the sky, and requires no real-time dynamical focus measurements. The telescope and AO system are first 'tuned', or optimized, on a nearby star, which calibrates the altitude of the sodium layer. This altitude is then kept fixed for the duration of the science observation. The galaxy is acquired, and the nucleus is used to measure tip/tilt while the higher-order atmospheric distortions are measured from the laser beacon. The open-loop model controls the changes in focus as the expected distance to the sodium layer changes. (Note that the distance from the telescope to the sodium layer changes as the object is tracked on the sky, even if the altitude of the sodium layer is fixed.)

4. APPLICATION TO GALAXY DYNAMICS**

4.1 NIFS Stellar Kinematics

We used this technique together with the NIFS integral-field spectrograph to measure the stellar kinematics around the nucleus of two nearby early-type galaxies. Figure 1 shows the measured stellar kinematic maps for the two galaxies, NGC524 and NGC2549, which were observed for 3.5 and 2.5 hours respectively on-source (i.e. excluding blank sky fields). Neighboring spectra have been binned together in the outer regions where the galaxy is fainter to ensure a minimum signal-to-noise ratio of around 50 in each spectrum. The central spectra have higher signal and are unbinned, thus preserving the spatial information delivered by the LGS-AO. This excellent data quality allows the higher-order moments of the velocity distribution to be measured, using a 6th-order Gauss-Hermite series. The higher-order moments are essential to derive the detailed orbital make-up around the black hole. We combine the NIFS data with wide-field integral field kinematics of comparable quality, but lower spatial resolution, from the SAURON spectrograph⁴ at the William Herschel Telescope (not shown).

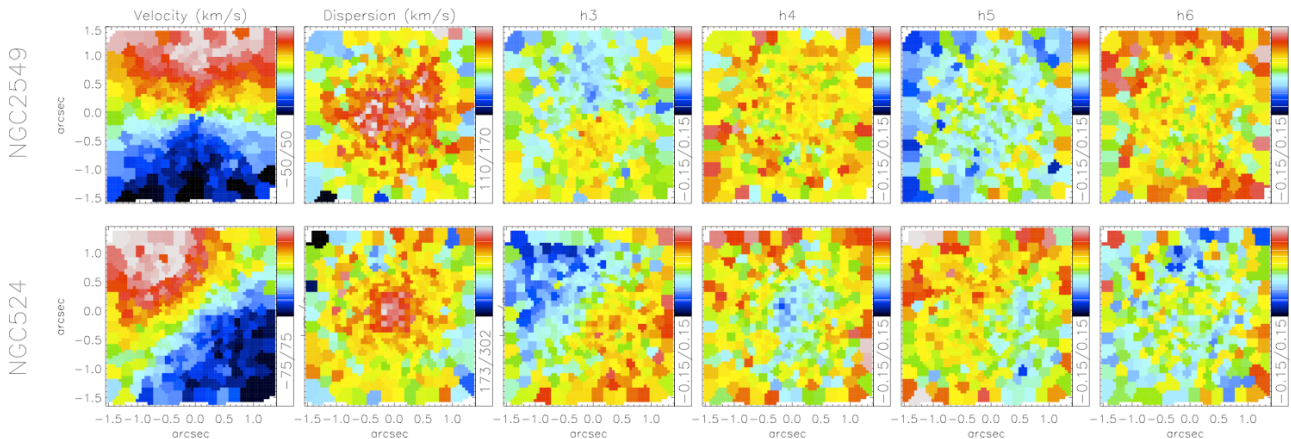


Figure 1. NIFS stellar kinematic maps for NGC2549 (top) and NGC524 (bottom). The velocity profile is parameterized by the standard Gauss-Hermite series, giving the mean velocity, V , the velocity dispersion, σ , and higher-order moments h_3 to h_6 . Note the observed rotation, the central increase in σ , and the anti-symmetric signatures in the higher moments. The data are spatially binned with a threshold signal-to-noise ratio of 50.

4.2 PSF Analysis

To estimate the degradation of the point-spread function (PSF) due to the use of the open-loop model, we took NIFS observations of the star used to tune the AO system both before the galaxy was observed (where all loops were optimised) and after approximately one hour of galaxy observations (with the focus loop left open, as for the galaxy). Figure 2 compares the PSFs derived from these observations, which show negligible degradation due to changes in the sodium layer or errors in the open-loop model. This is only one instance, of course, and the sodium layer altitude depends on the weather conditions for a given night. However it seems that this mode gives a reliable performance, at least over timescales of around an hour.

We must also estimate the PSF for our science data, since the tip/tilt information from the galaxy nuclei will not be as accurate as for a star of comparable brightness, because the galaxy has a more diffuse profile. We are also adding together hours of observations taken over several nights, and thus have to average over varying conditions, not to mention the errors in registering the individual images before adding them together. To estimate the actual delivered PSF, we compare the broad-band images of our galaxies (made by integrating the spectra in the NIFS data cubes) with archival HST images. By deriving the PSF required to smooth the HST image until it matches the resolution of the NIFS data, one can obtain an estimate of the PSF. This assumes there is no strong change in colour between the NIFS and HST spectral range, and that the HST PSF is negligible compared to the NIFS data. The galaxies in question are relatively free of dust, and we do not expect differences between the HST F814W filter and the NIFS K-band image to create a strong bias. We also found that in practice, the HST images have sufficiently higher spatial resolution than the combined NIFS data to make the HST PSF effectively negligible.

**Results summarized in this section are presented fully in [3]

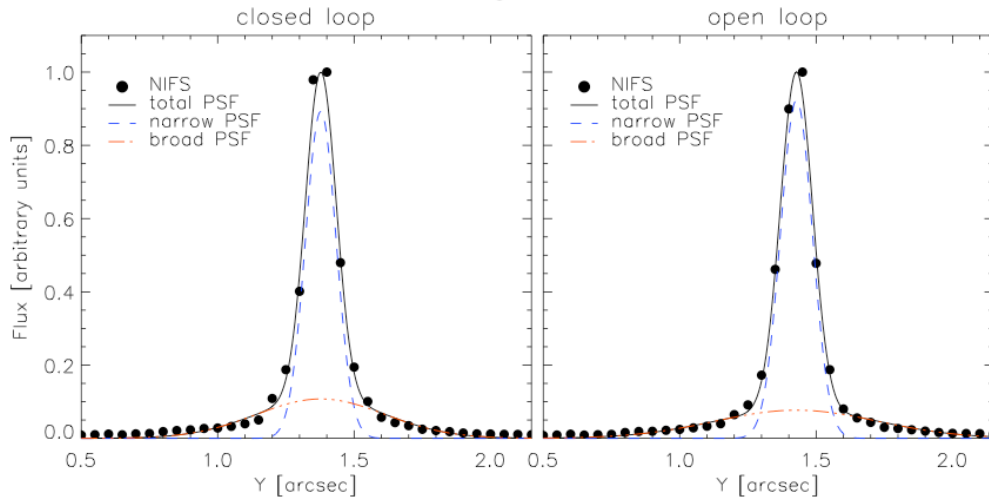


Figure 2: Comparison of the NIFS PSF derived from a star close to NGC524 used to tune the telescope and AO system. The observations were made before (left) and after (right) observing the galaxy. The ‘after’ images were taken without recalibrating the sodium layer altitude. This indicates any degradation due to using the open-loop focus model. The parameters of the double-Gaussian fit used to parameterise the NIFS PSF are almost identical, showing that no significant degradation occurred.

Figure 3 shows the encircled energy of the PSFs derived for the two galaxies. For NGC2549, 50% of the flux is kept within less than 0.2 arcseconds. For NGC524, 50% of the energy is within around 0.3 arcseconds. Note that NGC524 has a more shallow central light profile, whereas NGC2549 has a steep central light cusp, resulting in a better tip/tilt correction. The radius of influence for NGC2549 is significantly smaller than for NGC524 (0.05 arcseconds for NGC2549 versus 0.6 arcseconds for NGC524), so the improved PSF helps our sensitivity to the black hole.

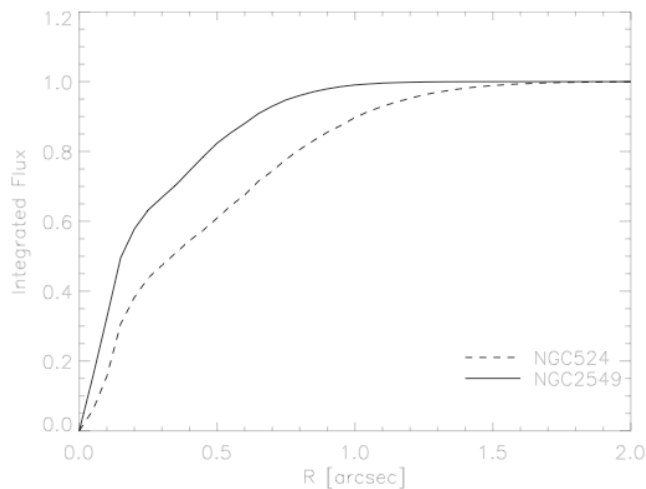


Figure 3: Encircled energy of the PSFs derived from the combined NIFS data on NGC2549 and NGC524. NGC2549 shows a more concentrated PSF, probably because its steeper central light profile provides a better tip/tilt correction.

4.3 Dynamical modeling

To infer the mass of the black hole from the stellar orbits around it requires a dynamical model of the galaxy. The mass and distribution of the galaxy's stars is modeled using imaging (HST combined with ground-based imaging), converted to mass via the mass-to-light ratio: a free parameter in the dynamical model. In addition to this, a central dark mass is included, which represents the black hole, and gives another free parameter. Lastly, the angle at which the galaxy is viewed must be assumed, since the shape of the galaxy we see is a two-dimensional projection on the sky of a three-dimensional body. The objects we are modeling are well described by a galaxy symmetric about its axis of rotation, for which the viewing direction is uniquely described by the inclination of the system. For both galaxies, good estimates of this inclination angle are available, so we assume these fixed values. Dark matter is included in the model implicitly through the mass-to-light ratio, making the assumption that the dark matter is distributed in the same way as the starlight. In practice, dark matter is not expected to dominate the stellar dynamics in the central regions of these galaxies.

Figure 4 shows the results of our modeling. The contours show the goodness of fit criterion plotted against the two free parameters of the model: mass-to-light ratio and black hole mass. Each dot represents a single dynamical model, which has been optimally fitted to the data for the given gravitational potential. At each dot, several thousand stellar orbits have been calculated, and the optimal combination of orbits that fit the kinematic data are found, requiring several hours of computing time.

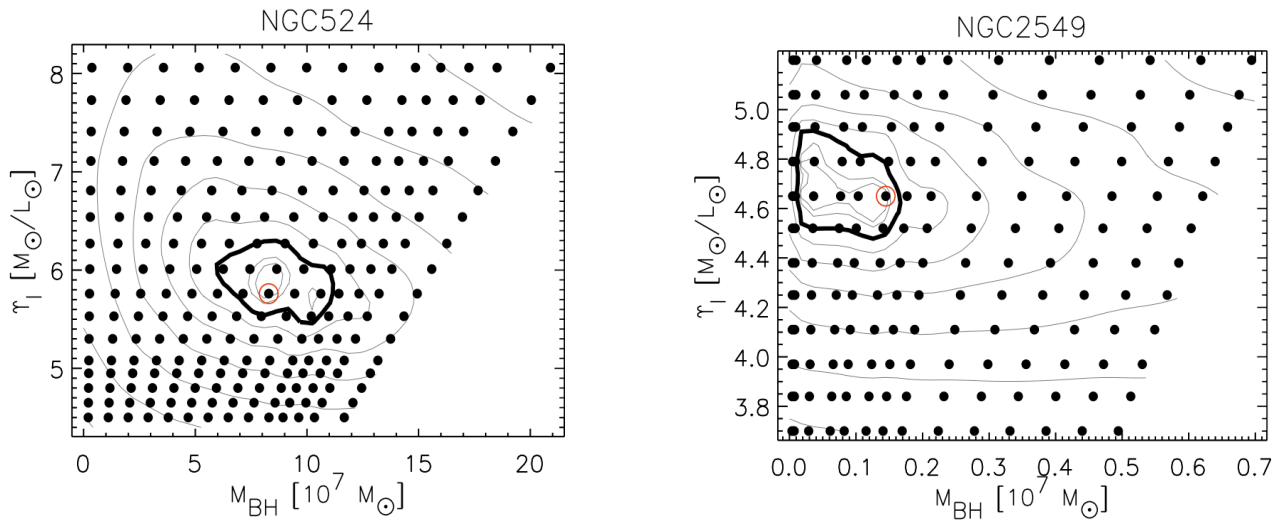


Figure 4: Contours showing the goodness of fit for the dynamical models of NGC524 (left) and NGC2549 (right) as a function of the free parameters: the mass-to-light ratio and the mass of the black hole. Each dot represents a fit of several thousand orbits to the NIFS and SAURON stellar kinematics and mass model, finding the best combination of orbits for the given gravitational potential. Thick contours indicate the 3σ confidence level.

The thick contour in each plot shows the 99.9% confidence level, inside of which lies the best-fitting model. In both cases, the model with no black hole is excluded at this confidence level. Figure 5 shows a comparison of the central velocity dispersion from NIFS (generally the most sensitive tracer kinematic of the black hole) with that of the fit from the best-fitting model, as well as a model with a much smaller and a much larger black hole. Whilst most of the field is unchanged between the different models, the very central regions of the NIFS data show variations. It is these subtle differences that indicate the presence and mass of the central black hole.

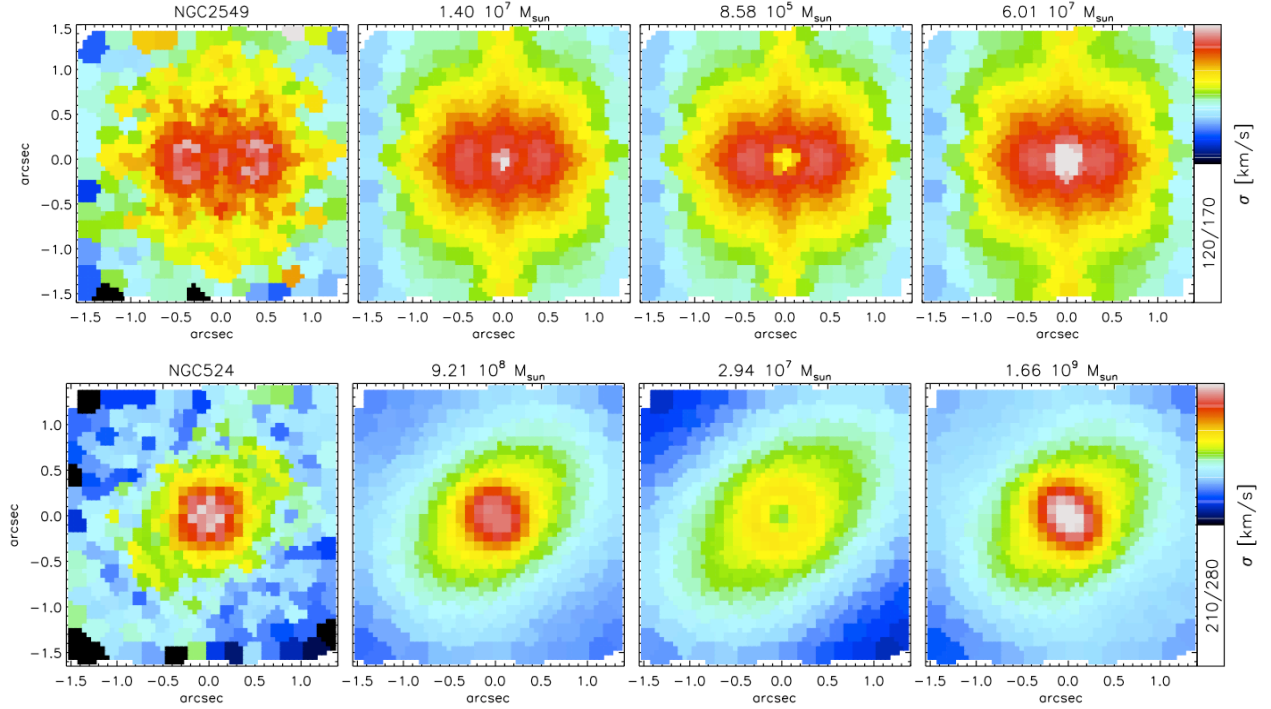


Figure 5: Comparison of the observed NIFS velocity dispersion (left column) and the best-fitting model (second to left column) for NGC2549 (top) and NGC524 (bottom). Models with too small and too large a black hole (second from right and right columns respectively) are also shown for comparison. Note how only the central pixels differ significantly.

Thanks to the high-quality NIFS data coupled with our general dynamical modeling, we can also infer the orbital structure close to the black hole. Figure 6 shows a measure of the balance between radial and tangential orbits in the galaxy. NGC524 shows a very distinct change inside the black hole radius of influence towards tangential anisotropy, meaning a relatively higher fraction of orbits going around the galaxy centre than passing through it. This is compelling evidence that the central core region of this galaxy was formed by a black hole binary following a galaxy merger, which ejected the central stars that were on radial orbits, leaving a depleted core region biased to tangential orbits. The picture for NGC2549 is less clear, with only weak evidence for any change in anisotropy close to the black hole. This may suggest that this galaxy, which shows a steep central light profile and no core, has no such tangential bias, indicating a different formation history to NGC524. We note that the spatial resolution of the NGC2549 data relative to the radius of influence is poorer than for NGC524, however, and that the lack of significant signatures in the anisotropy for this galaxy may be due to relatively less spatial information.

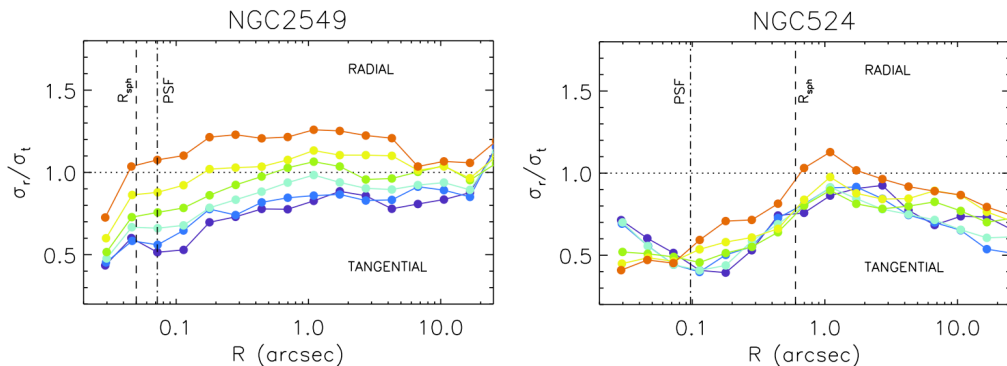


Figure 6: Radial profiles showing the balance between radial and tangential orbits for NGC2549 (left) and NGC524 (right). Coloured lines indicate different angles from the equatorial plane, increasing from red to blue. Dotted lines indicate the width of the PSF core, and the dot-dash lines show the radius of influence. NGC524 shows a strong tangential anisotropy within the radius of influence. NGC2549 shows a less strong trend, but the radius of influence is not as well resolved.

4.4 Conclusions

Using the open-loop focus model technique, LGS-AO at Gemini has allowed unique, high-quality spectral maps of these galaxy nuclei to be made at very high spatial resolution. These observations have revealed the presence of a super-massive black hole residing at the centre of each galaxy. More importantly, they provide evidence that early-type galaxies with different central light characteristics (cusps and cores) have correspondingly different orbital structures, indicative of distinct formation scenarios. This adds new insight into the connections between super-massive black holes, galaxy nuclei, and the evolution of early-type galaxies.

5. FUTURE DEVELOPMENTS: PERIPHERAL GUIDING WITH LGS[†]

At Gemini North we have recently tested the use of the standard ‘peripheral’ wave-front sensor to provide off-axis tip/tilt correction in combination with the on-axis LGS for higher-order modes. This provides access to some amount of AO correction across a much larger fraction of the sky, since the patrol field of the peripheral guider is significantly larger than that of the Altair AO system alone. Tip/tilt correction is performed ‘closed-loop’ by the telescope’s secondary mirror at speeds up to 200 Hz. For the purpose of testing, focus corrections are made via the open-loop model described above, but ultimately the focus will also be corrected closed-loop.

Figure 7 shows some preliminary results from these tests. The quality of correction is naturally much reduced over on-axis performance, which is primarily caused by the limitation of the large off-axis distance to the tip/tilt star (typically around 6 arcminutes), as well as the lower responsiveness of the secondary mirror for fast tip/tilt corrections. However, the PSF is significantly improved over natural seeing, giving a factor 2-3 improvement in terms of FWHM, with corresponding increases in peak signal-to-noise ratio. For spectroscopic studies, where raw flux concentration is usually more important than the delivered image quality, this additional gain encircled energy is significant. This is especially true for studies of high-redshift galaxies, where concentrating as much flux onto as few pixels as possible is the most important consideration.

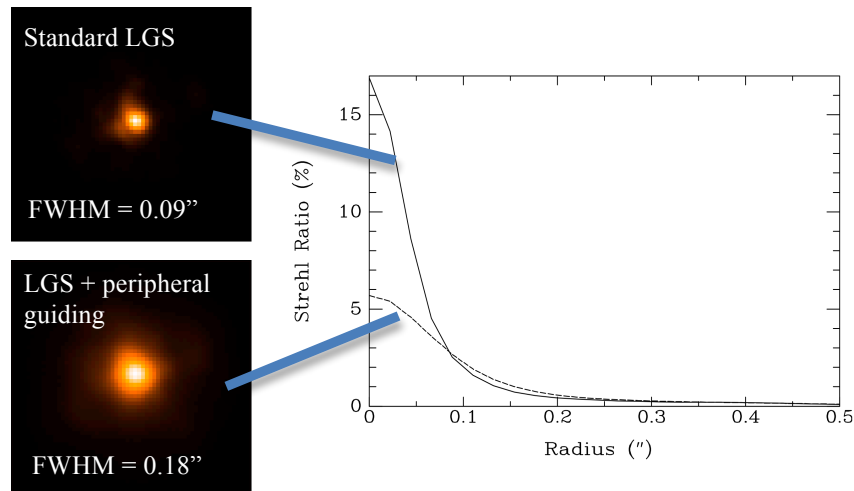


Figure 7: *Left images:* Comparison of image quality delivered by the current on-axis LGS system (top) and using a 6 arcminute off-axis peripheral guide star via the standard telescope guide system (bottom). The natural seeing in both cases was around 0.6". *Right panel:* Comparison of the point-spread function (PSF) from these two modes, normalized by their Strehl ratios (indicated by the y-axis).

[†] See related presentation by J. Christou at this conference

This new mode gives greatly increased sky coverage. Figure 8 shows the sky coverage predictions for different LGS modes at Gemini North. The current offered LGS mode is shown by the black line, which does well at low galactic latitudes by virtue of the high stellar density. However, at high latitudes, the sky coverage drops dramatically. Such locations, however, are the primary sites for deep-field studies of high-redshift galaxies. The green line shows the expectations for the current peripheral wavefront sensor used for the tests, which is not currently optimized for this task. We are planning to install a dichroic filter to eliminate background light from the laser, and a 2x2 Shack-Hartmann to replace the current 8x8 system, which will significantly increase the limiting magnitude of the wavefront sensor, pushing sky coverage up towards 100% (red curve). In addition, this mode will allow AO-corrected observations of low-contrast extended sources, such as nearby giant galaxies, for which AO correction is not possible otherwise. We anticipate this ‘seeing improver’ mode to be offered for scientific use in 2011.

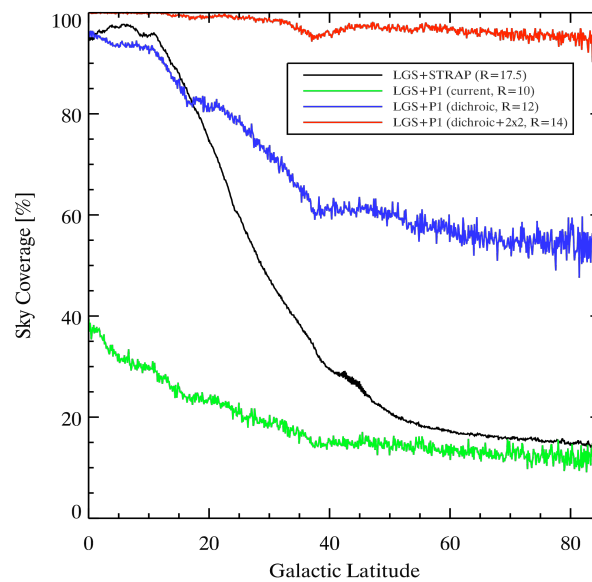


Figure 8: Sky-coverage estimates for the current LGS configuration (black), test configuration with peripheral guiding (green), and future peripheral guiding mode with upgraded optics (blue and red). See main text for details.

ACKNOWLEDGEMENTS

Based on observations obtained at the Gemini Observatory, which is operated by the Association of Universities for Research in Astronomy, Inc., under a cooperative agreement with the NSF on behalf of the Gemini partnership: the National Science Foundation (United States), the Science and Technology Facilities Council (United Kingdom), the National Research Council (Canada), CONICYT (Chile), the Australian Research Council (Australia), Ministério da Ciência e Tecnologia (Brazil) and Ministerio de Ciencia, Tecnología e Innovación Productiva (Argentina).

REFERENCES

- [1] Ferrarese, L., & Ford, H. 2005, *Space Science Reviews*, 116, 523
- [2] Rees, M.J. 1984, *Annual Review of Astronomy and Astrophysics*, 22, 471
- [3] Krajinovic, D., McDermid, R.M., Cappellari, M., & Davies, R.L. 2009, *MNRAS*, 399, 1839
- [4] Bacon, R., et al. 2001, *MNRAS*, 326, 23